

LOADING OF A KRYPTON MAGNETO-OPTICAL TRAP WITH TWO HOLLOW LASER BEAMS IN A ZEEMAN SLOWER

S. Singh, V. B. Tiwari, S. R. Mishra, H. S. Rawat*

*Laser Physics Applications Section,
Raja Ramanna Centre for Advanced Technology,
Indore-452013, India*

Received April 11, 2014

A significant enhancement in the number of cold atoms in an atomic-beam-loaded magneto-optical trap (MOT) for metastable krypton atoms is observed when hollow laser beams are used in a Zeeman slower instead of a Gaussian laser beam. In the Zeeman slower setup, a combination of two hollow laser beams, i. e., a variable-diameter hollow beam generated using a pair of axicon lenses superimposed on a fixed-diameter hollow beam, has been used to reduce the longitudinal velocity of the atoms in the atomic beam below the capture speed of the MOT. The observed enhancement in the number of atoms in the MOT is attributed to reduced destruction of the atom cloud in the MOT and increased cooling of the off-axis atoms in the atomic beam, resulting from the use of hollow beams in the Zeeman slower.

DOI: 10.7868/S0044451014090065

1. INTRODUCTION

The laser cooling of noble gas atoms in the excited state is an attractive area of research to study cold atom collisions, ionization physics, nanolithography, and atom trap trace analysis (ATTA) [1, 2]. Compared to alkali atoms, which are cooled in the ground state, noble gas atoms are laser cooled in a metastable excited state. The excitation to this metastable state can be achieved by radio-frequency (RF) excitation [3, 4]. The metastable state atoms generated in the discharge section are transported to the magneto-optical trap (MOT) chamber in the form of an atomic beam. Capturing these atoms in the MOT requires reducing the longitudinal velocity of the atoms in the atomic beam below the capture velocity of the MOT. A high flux of the slowed metastable atoms in the atomic beam is important for efficient loading of the MOT, which is a workhorse for many experiments including Bose–Einstein condensation (BEC), atom optics, and atomic physics [5, 6]. The slowing of the atomic beam is conveniently achieved by using a Zeeman slower device [7], which is used as a decelerating unit for the atomic beam before its entry to the MOT chamber. The Zeeman slower decelerates the atoms through Doppler laser

cooling of atoms in the presence of a spatially varying magnetic field. The deceleration results from the scattering force on an atom due to a laser beam propagating opposite to the atomic beam direction. The variation of the magnetic field in the Zeeman slower is kept in such a way that the Zeeman shift in the atomic transition frequency compensates the Doppler shift in the laser frequency for a moving atom. Thus, laser beam interacts resonantly with the atoms throughout the length of the Zeeman slower, which leads to effectively slowing the atomic beam for the loading of the MOT.

In a Zeeman slower based atomic-beam-loaded MOT, a known difficulty is the destruction of the MOT atom cloud by the Zeeman slower laser beam, as the MOT cloud is formed on the atomic beam axis to which the Zeeman slower laser beam is aligned from the opposite direction. This laser beam, being close to the resonance with the atomic transition, thus knocks out the trapped atoms from the MOT at its higher power. This perturbation to the MOT cloud can be reduced by the off-axis alignment of the Zeeman slower laser beam such that the MOT cloud does not come in the way of the laser beam. But this also results in a decrease in the number of atoms in the MOT due to poor loading of the MOT caused by the less effective cooling in the Zeeman slower. In an important work [8], this problem was tackled by using a hollow Zeeman slower laser beam

*E-mail: surendra@rrcat.gov.in

aligned axially opposite to the atomic beam, such that the MOT cloud was formed in the dark central region of the hollow beam. The hollow beam was generated by using a dark spot in the central region of the transverse cross section of a Gaussian beam. This resulted in an enhancement in the number of atoms accumulated in the MOT. In another work [9], the decelerating Zeeman slower laser beam was tightly focused at a position slightly away (in the transverse direction) from the MOT cloud, such that its perturbation to the MOT cloud was as small as possible. But in this geometry, the number of atoms is expected to be very sensitive to the position of the focus of the Zeeman slower beam.

In this paper, we use two hollow laser beams of different dark diameters and ring widths in the Zeeman slower of an atomic-beam-loaded krypton MOT. The first hollow beam is generated using a dark spot in the path of a Gaussian beam. With this hollow beam used as a Zeeman slower beam, the observed enhancement in the number of atoms in the MOT is $\approx 30\%$ of the number observed with a Gaussian Zeeman slower beam of same power. With the use of an additional second hollow beam of a larger dark diameter, we observe a further enhancement by $\approx 30\%$ in the number of cold atoms in the MOT. This enhancement in the number of atoms in the MOT is attributed to more efficient cooling of the off-axis atoms in the atomic beam due to a specific intensity profile of the second hollow beam. Thus, combining two hollow beams in the Zeeman slower results in a larger number of atoms in the MOT cloud due to more efficient cooling of the atomic beam with lesser destruction of the MOT cloud compared with the use of a regular Gaussian beam in the Zeeman slower.

2. EXPERIMENTAL SETUP

The schematic of our experimental setup for the generation of two hollow beams for the Zeeman slower is shown in Fig. 1. The first hollow beam was a fixed-diameter hollow beam (HB1) generated by keeping a transparent glass slide with a dark spot in the path of a Gaussian laser beam from an extended cavity diode laser (ECDL) system having the maximum power of ≈ 50 mW. The optimum size of the dark spot to generate HB1 was found by varying the size of the dark spot for a given ≈ 30 mW power in the beam (before the dark spot) and measuring the number of atoms in the MOT with the HB1 beam used in the Zeeman slower. The optimum size of the dark spot was ~ 1 mm, and hence HB1 with this dark spot was used in further ex-

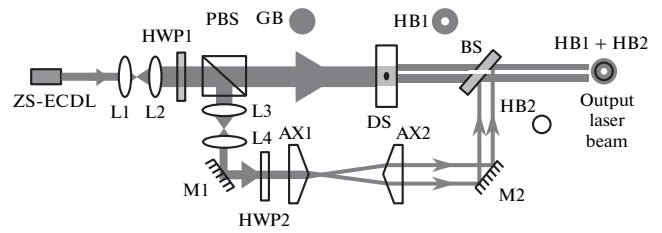


Fig. 1. Schematic of the experimental setup for the generation of hollow beams. ZS-ECDL — Zeeman slower-extended cavity diode laser; L1, L2, L3, and L4 — lenses of appropriate focal lengths; HWP1 and HWP2 — half-wave plates; PBS — polarizing beam splitter cube; GB — Gaussian beam; DS — dark spot on the transparent glass plate; BS — beam splitter; M1 and M2 — mirrors; AX1 and AX2 — axicon lenses; HB1 — hollow beam generated using the dark spot; HB2 — hollow beam generated using the axicon lenses

periments. The second hollow beam was a variable-diameter hollow beam (HB2) generated by taking a part of a laser beam and passing it through a pair of axicon lenses (with the cone angle 176°) mounted on a calibrated translation stage (Fig. 1). These lenses were facing each other in the path of the slowing laser beam [10]. The dark diameter of the hollow beam (d) can be varied by varying the separation between the axicon lenses, similarly to an earlier work that used a pair of axicon mirrors to generate a variable-diameter collimated hollow beam [11].

The experiments reported here were performed on our magneto-optical trap setup for metastable Kr atoms, which is also described elsewhere [12]. The schematic of this experimental setup for cooling and trapping of $^{84}\text{Kr}^*$ atoms is shown in Fig. 2. The krypton gas first flows into the RF discharge glass tube through the inlet chamber (C1) with the pressure $\sim 10^{-3}$ Torr. The glass tube has the inner diameter of 10 mm and the length of 150 mm. The Kr^* atoms produced in this tube by the RF-driven discharge (frequency ≈ 30 MHz) pass through the analysis chamber (C2) with the pressure $\sim 10^{-5}$ Torr. A Zeeman slower (length ≈ 80 cm) along with an extraction coil was connected between the pumping chamber (C3) with the pressure $\sim 10^{-6}$ Torr and the MOT chamber (C4) with the pressure $\sim 10^{-8}$ Torr. It slows down the $^{84}\text{Kr}^*$ atomic beam before cooling and trapping in the MOT chamber. The Zeeman slower laser beam that we used was composed of two hollow beams as shown in Fig. 1. This laser beam propagates opposite to the atomic beam and is σ^+ polarized. Its frequency was de-

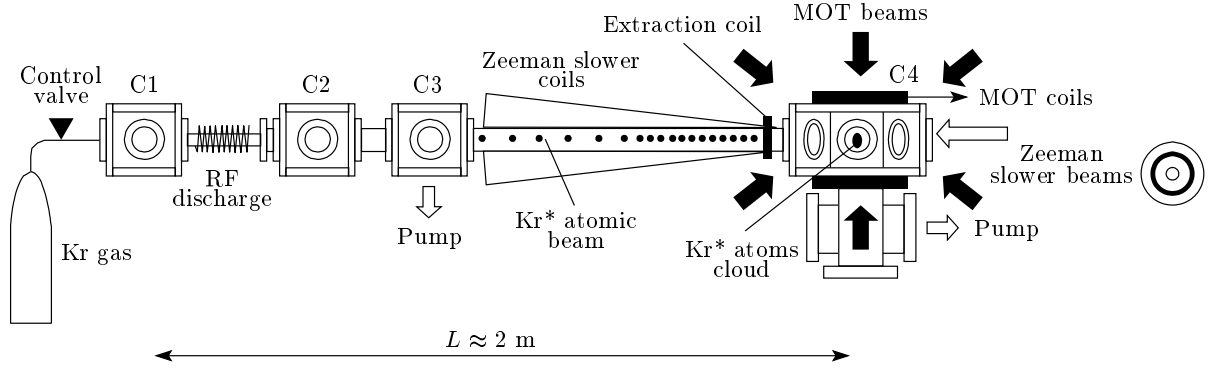


Fig. 2. Schematic of the experimental setup for cooling and trapping metastable Kr atoms. C1 — inlet chamber (10^{-3} Torr), C2 — analysis chamber (10^{-5} Torr), C3 — pumping chambers (10^{-6} Torr), C4 — MOT chamber (10^{-8} Torr)

tuned by ≈ 80 MHz to the red of the $^{84}\text{Kr}^*$ transition between $5s[3/2]_2$ and $5p[5/2]_3$ states. The cooling laser beam for the MOT was split into three beams, each having a power of ≈ 5 mW (the $1/e^2$ radius ≈ 3 mm). These beams were used in a retro-reflection geometry to obtain the desired six beams for the MOT. The frequency of the MOT cooling laser was kept at ≈ 6 MHz red-detuned to the $5s[3/2]_2 \rightarrow 5p[5/2]_3$ transition of $^{84}\text{Kr}^*$. A pair of anti-Helmholtz magnetic coils provided the magnetic field gradient of ~ 10 G/cm for the MOT formation.

In the Zeeman slower, the magnetic field variation along the atomic beam direction was designed to provide an effective cooling of the longitudinal velocity of an atomic beam. In the magnetic field of the Zeeman slower, the Zeeman-shifted atomic transition frequency is equal to the Doppler-shifted frequency of the counter-propagating laser beam. This resonance condition can be expressed as $\omega_0 + \mu_B B_z / \hbar = \omega_L + kv$, where ω_0 is the atomic transition frequency without any magnetic field, ω_L is the slower laser frequency, μ_B is the Bohr magneton, B_z is the axial magnetic field in the Zeeman slower at the distance z from the entrance to the Zeeman slower, and v is the longitudinal speed of an atom interacting with the Zeeman slower laser beam. The effective detuning of the slower laser beam from the atomic transition can be written as

$$\Delta = \omega_L - \omega_0 + kv - \frac{\mu_B B_z}{\hbar}. \quad (1)$$

To know the longitudinal velocity of an atom at the boundary of the MOT trapping region, the initial velocity and deceleration in the Zeeman slower are important parameters. The deceleration $a(z, r)$ of an atom in the Zeeman slower at the longitudinal distance z and transverse distance r is given as

$$F(z, r) = ma(z, r) = \hbar k \frac{\Gamma}{2} \frac{I_{zs}(r)/I_s}{1 + I_{zs}(r)/I_s + 4(\Delta/\Gamma)^2}, \quad (2)$$

where $F(z, r)$ is the scattering force, m is the mass of the $^{84}\text{Kr}^*$ atom, $k = 2\pi/\lambda$, where λ is the wavelength, $\Gamma (= 2\pi \cdot 5.56$ MHz) is the line width, I_s is the saturation intensity (for the $^{84}\text{Kr}^*$ atom, $I_s = 1.36$ mW/cm 2), and $I_{zs}(r) = I_0 \exp(-2r^2/\sigma_0^2)$ is the transverse intensity profile of the Zeeman slower laser beam. Here, r and σ_0 denote the transverse position and the beam spot size. This deceleration $a(z, r)$ governs the variation in the longitudinal velocity with the distance z as

$$v(z + \delta z)^2 = v(z)^2 - 2a(z, r) \delta z, \quad (3)$$

where $v(z)$ and $v(z + \delta z)$ are the velocities at distances z and $z + \delta z$ in the Zeeman slower. For the changing values of $v(z)$, the variation of B_z with z is required so as to keep the detuning (Δ) minimum to achieve maximum deceleration throughout the length of the Zeeman slower.

The role of the extraction coil is to tailor the B_z field such that the longitudinal velocity of atoms be low outside the Zeeman slower in the MOT chamber. This facilitates the atoms reaching the capture volume of the MOT and being trapped in the MOT. The currents in the Zeeman slower and extraction coils were optimized independently to obtain the maximum flux of the slowed atoms in the MOT chamber. Figure 3 shows the simulated and measured magnetic field profile along the length of the Zeeman slower.

An overlap of the MOT beams forms the trapping region. For an atom approaching the trap to be finally cooled and trapped, it is important that its longitudinal velocity at the entry point of the trapping region be smaller than the capture velocity $V_c = \sqrt{\hbar k \Gamma / 2m}$

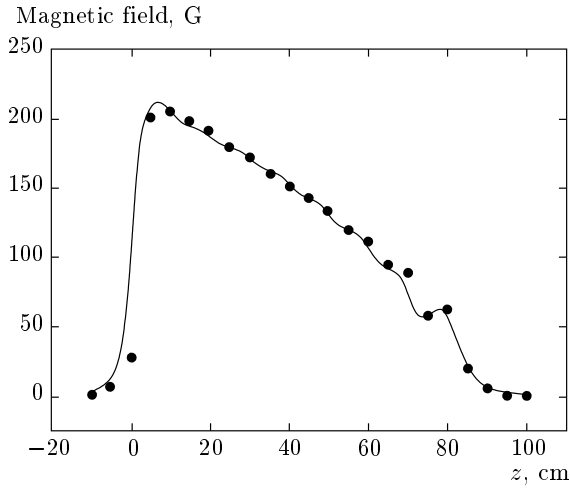


Fig. 3. Variation of the magnetic field in the Zeeman slower with axial distance. The continuous curve shows the simulated field for a 1.3 A current in the Zeeman slower coil and a 3.5 A current in the extraction coil. The dots represent the measured magnetic field due to both these coils at these values of the currents in the Zeeman slower

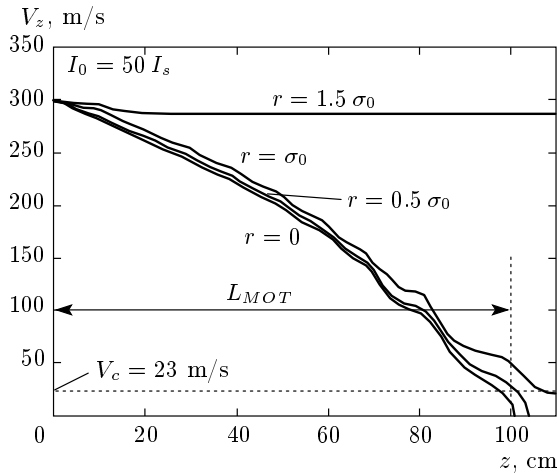


Fig. 4. The theoretically calculated variation in the speed of the atoms along the axial distance (z) of the Zeeman slower for a Gaussian slower beam $I_{zs}(r) = I_0 \exp(-2r^2/\sigma_0^2)$. Here, I_0 is the peak intensity, σ_0 is the beam waist radius, I_s is the saturation intensity, V_c is the capture velocity, and L_{MOT} is the distance of the boundary of the MOT trapping region from the Zeeman slower entrance

of the MOT, where l is the radius of the trap [13]. For a Gaussian Zeeman slower beam, the calculated variation in the longitudinal velocity of the atom with the distance z is shown in Fig. 4. It is evident from

Fig. 4 that the final longitudinal velocity of the atom depends on its transverse position. For an atom moving with the initial longitudinal velocity ≈ 300 m/s (at $z = 0$) along the atomic beam axis (i. e., $r = 0$), opposite to a Gaussian Zeeman slower beam with the peak intensity $I_0 = 50I_s$, the final velocity of the atom at $z = L_{MOT}$ (i. e., at the boundary of the MOT trapping region) reduces to a value lower than the capture velocity of the MOT ($V_c = 23$ m/s). However, the final longitudinal velocity remains significantly larger than V_c if the atom is positioned at the transverse distance $r = \sigma_0$. This clearly shows that atoms moving off-axis are not cooled to a velocity lower than V_c by a Gaussian-profile Zeeman slower beam. An increase in power in a Gaussian beam for the effective cooling of off-axis atoms is expected to lead to the destruction of the MOT. Therefore, we considered the preferential increase in the off-axis intensity in the Zeeman slower beam. This was implemented by using multiple hollow beams of different dark diameters for the Zeeman slower cooling. This helps keep the high off-axis intensity in the Zeeman slower beam for the effective cooling of the atomic beam, along with the low on-axis intensity for less destruction of the on-axis MOT cloud.

In order to test the appropriate working of the Zeeman slower, we measured the longitudinal velocity of atoms in the atomic beam after the Zeeman slower. Figure 5a shows the schematic of the experimental setup used for the measurement of the velocity of $^{84}\text{Kr}^*$ atoms by the light induced fluorescence method. Two probe laser beams (probe 1 and probe 2) generated from the same ECDL crossing the atomic beam at 90° and 45° angles were used to excite $^{84}\text{Kr}^*$ atoms and generate the fluorescence signals.

In Fig. 5b, curve I shows the fluorescence signal from the atomic beam due to both the probe beams simultaneously (i. e., probe 1 and probe 2, which are at the angles of 90° and 45° to the Kr^* atomic beam propagation direction), whereas curve II shows the fluorescence signal only due to the probe beam at the 45° angle (i. e., probe 2), with a Gaussian intensity profile laser beam used in the Zeeman slower. Curve II in Fig. 5b shows the longitudinal velocity profile of the slowed atomic beam after the Zeeman slower. The position of the peak in the signal in this figure can be used to estimate the longitudinal velocity of the atoms at the exit from the Zeeman slower. Corresponding to the main peak shown in curve II in Fig. 5b, the longitudinal velocity of atoms in the atomic beam is ≈ 15 m/s. The width of this peak shows that the full width at half maximum (FWHM) of the longitudinal velocity distribution is ≈ 30 m/s. This width of the velocity profile is due

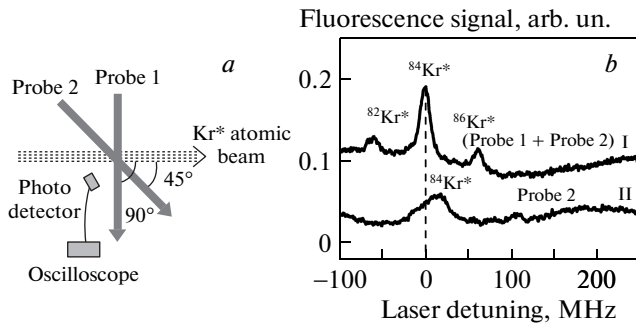


Fig. 5. *a)* The schematic of the experimental setup for the measurement of the speed of an atomic beam. *b)* Typical fluorescence signals as a function of laser detuning when two probe laser beams (probe 1 and probe 2) cross the atomic beam simultaneously with Zeeman slower beam off (curve I), and when only probe 2 crosses the atomic beam with Zeeman slower beam on (curve II)

to several reasons, which include the spatial variation in the slowing laser beam intensity and variation in the magnetic field of the Zeeman slower [14]. In our experiments, the number of atoms accumulated in the MOT was estimated by the fluorescence imaging method after collecting the fluorescence from the MOT cloud with a CCD camera [15, 16]. Also, the hollow beam (HB2) diameter was varied by varying the separation between the axicon lenses.

3. RESULTS AND DISCUSSION

In order to investigate the role of the transverse intensity profile of the Zeeman slower laser beam on the MOT loading, we first used the HB1 beam and observed the number of atoms in the MOT. The number in the MOT was maximized by varying the size of the dark spot in this beam (HB1) at a fixed input beam power of 30 mW. As shown in Fig. 6, the maximum number was obtained with the dark spot 1 mm size. This size of the dark spot was used in further experiments with the HB1 beam.

Figure 7 compares the performance of a Gaussian and a hollow laser beam (HB1) used in the Zeeman slower. For the data shown in Fig. 7, the power in the Gaussian beam was measured before the entrance to the chamber. For the exact comparison with the Gaussian beam, the power in HB1 was also measured at the same place (i. e., after the dark spot position). We observed that the use of HB1 as the Zeeman slower laser beam always resulted in a higher number of atoms in the MOT than the number obtained with the Gaussian profile slower laser beam (Fig. 7, curves *a* and *b*). This

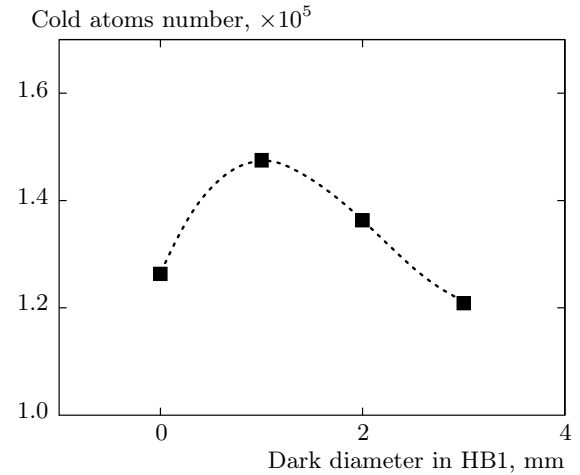


Fig. 6. Measured variation in the cold-atom number in the MOT with the dark spot diameter of the hollow beam HB1. The dotted line is guide to the eye

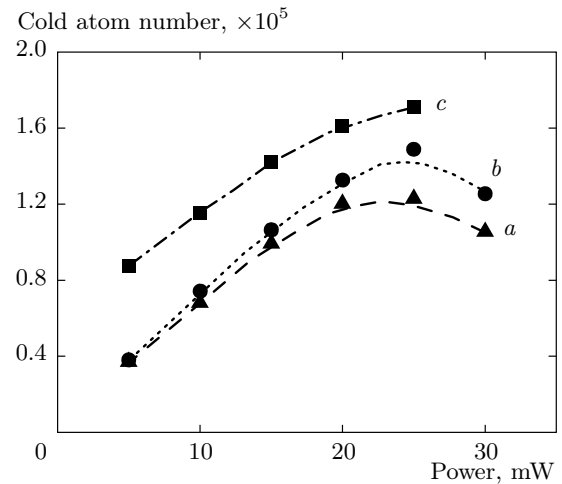


Fig. 7. The measured variation in the cold atom number in the MOT with the power of the Zeeman slower laser beam. Curve *a* is for the power in the Gaussian beam and curves *b* and *c* are for the power of the hollow beam HB1 (dark spot diameter 1 mm). Curve *c* shows the variation in the number with the power in the HB1 beam in the presence of the HB2 beam with a power of 5 mW. The powers in HB1 and HB2 were measured before their entrance into the MOT chamber.

The dashed lines are guide to the eye

observation is qualitatively similar to the one reported in [8]. However, the enhancement factor reported in Ref. [8] is much higher than that we observed. This could be possibly due to a much higher flux of atoms used in [8] for MOT loading with ground-state alkali

Na atoms. Our MOT is loaded from metastable Kr atoms with a much smaller flux than the flux used for alkali Na atoms.

Motivated by the simulations shown in Fig. 4, we then used an additional hollow beam with a larger dark diameter (HB2, as indicated in Fig. 1) in the presence of the HB1 Zeeman slower beam and measured the number of metastable Kr atoms in the MOT. Figure 7 (curve *c*) shows that with this additional beam, i. e., HB2 superimposed on the HB1 beam (with the dark diameter of 1 mm), the observed number of atoms in the MOT was higher than the number obtained with the single Zeeman slower beam HB1. This observed enhancement in the number of atoms in the MOT (curve *b* and curve *c* in Fig. 7) is attributed to a more efficient cooling of the off-axis atoms in the atomic beam due to the superposition of the HB2 beam. The enhancement can be further improved by increasing the power in HB2, which was limited to 5 mW in the present experiments due to sharing the total power by the HB1 and HB2 beams. The power and the diameter of the second hollow beam (HB2) was kept constant (power: 5 mW, inner diameter: 7 mm, outer diameter: 10 mm) for the measurements shown in Fig. 7. This size of HB2 was chosen after optimization of the number of atoms in the MOT with the HB2 diameter at the power of 5 mW (as shown in Fig. 8). We can also note from Fig. 8 that by increasing the ring width of the HB2 beam around the optimum value of the HB2 dark diameter, the number of trapped atoms can be further increased.

The improvement in the number of atoms in the MOT due to modification in the Zeeman slower beam intensity profile can be due to both effects, i. e., less destruction of the MOT cloud and an increased flux of slowed atoms for the MOT loading. To confirm the effect of the Zeeman slower beam profile on the flux of slowed atomic beam, the flux with hollow Zeeman slower beams was examined by measuring the fluorescence signal from the atomic beam. For this, the fluorescence signals due to a probe laser beam at 45° (probe 2) were recorded for the Gaussian laser beam as well as for the hollow laser beams (HB1+HB2) used in the Zeeman slower. The results are compared and shown in Fig. 9. Curve *a* in Fig. 9 shows the fluorescence signals for the Gaussian Zeeman slower beam having the power 30 mW, and curve *b* shows the fluorescence signal with the hollow slower beams HB1+HB2 with the respective powers 25 mW and 5 mW. The results evidently show that a higher flux is obtained with the hollow beams used in the Zeeman slower than that with a Gaussian beam of the same total power.

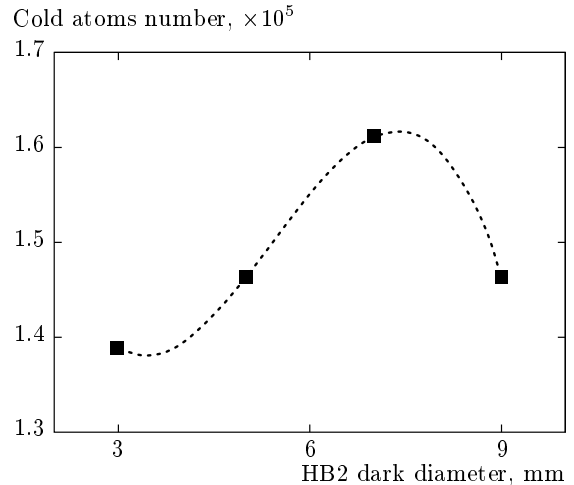


Fig. 8. The measured variation in cold atoms in the MOT with the HB2 dark diameter in the final Zeeman slower beam (HB1+HB2) for the respective powers 25 mW and 5 mW in HB1 and HB2 beams. The dotted line is guide to the eye

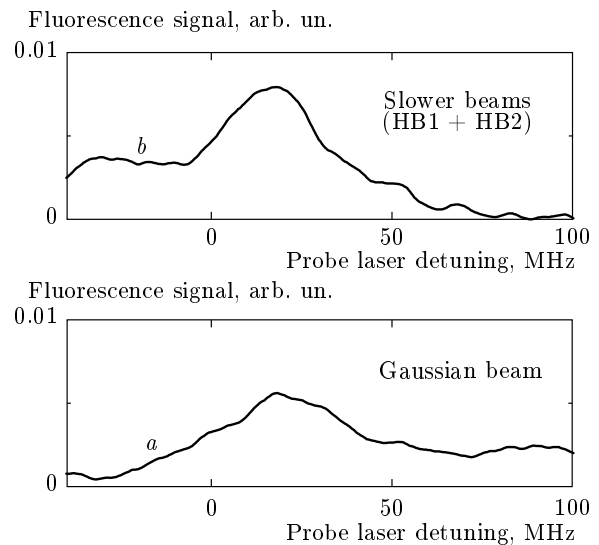


Fig. 9. The fluorescence signals due to the 45° probe beam (i. e., probe 2) alone as a function of the probe laser beam detuning; curve *a* is for a Gaussian profile of the slower laser beam of a 30 mW power, and curve *b* is for a combination of hollow slower beams (HB1+HB2) with the respective power 25 mW and 5 mW in HB1 and HB2

4. CONCLUSION

In conclusion, we report that a significant enhancement in the number of atoms in the MOT can be achieved by using two dark hollow beams in the Zeeman slower of an atomic-beam-loaded MOT. The enhancement in the number of atoms is attributed to the enhanced MOT loading due to efficient slowing of the off-axis atoms in the atomic beam and reduced destruction of the MOT by the hollow Zeeman slower beam.

We thank Y. B. Kale for his technical help during the experiments. We also thank S. P. Ram and S. K. Tiwari for various suggestions and help during the work.

REFERENCES

1. W. Vassen, C. Cohen-Tannoudji, M. Leduc et al., *Rev. Mod. Phys.* **84**, 175 (2012).
2. K. Bailey, C. Y. Chen, X. Du et al., *Nucl. Instr. Meth. B* **172**, 224 (2000).
3. C. Y. Chen, K. Bailey, Y. M. Li et al., *Rev. Sci. Instr.* **72**, 271 (2001).
4. J. Welte, F. Ritterbusch, I. Steinke, M. Henrich, W. Aeschbach-Hetig, and M. K. Oberthaler, *New J. Phys.* **12**, 065031 (2010).
5. W. Lu, M. D. Hoogerland, D. Milic, K. G. H. Baldwin, and S. J. Buckman, *Rev. Sci. Instr.* **72**, 2558 (2001).
6. J. A. Swansson, K. G. H. Baldwin, M. D. Hoogerland, A. G. Truscott, and S. J. Buckman, *Appl. Phys. B* **79**, 485 (2004).
7. W. D. Phillips and H. Metcalf, *Phys. Rev. Lett.* **48**, 596 (1982).
8. S. G. Miranda, S. R. Muniz, G. D. Telles, L. G. Marcassa, K. Helmerson, and V. S. Bagneto, *Phys. Rev. A* **59**, 882 (1999).
9. R. L. Cavasso Filho, D. A. Manoel, D. R. Ortega, A. Scalabrin, D. Pereira, and F. C. Cruz, *Appl. Phys. B* **78**, 49 (2004).
10. I. Golub and R. Tremblay, *J. Opt. Soc. Amer. B* **7**, 1264 (1990).
11. S. K. Tiwari, S. R. Mishra, S. P. Ram, and H. S. Rawat, *Appl. Opt.* **51**, 3718 (2012).
12. S. Singh, V. B. Tiwari, S. R. Mishra, and H. S. Rawat, *Laser Phys.* **24**, 025501 (2014).
13. A. M. Steane, M. Chowdhury, and C. J. Foot, *J. Opt. Soc. Amer. B* **9**, 2142 (1992).
14. P. N. Melentiev, P. A. Borisov, and P. A. Balykin, *Zh. Eksp. Teor. Fiz.* **125**, 761 (2004). [*JETP* **98**, 667 (2004).]
15. V. B. Tiwari, S. Singh, H. S. Rawat, and S. C. Mehendale, *Phys. Rev. A* **78**, 063421 (2008).
16. S. R. Mishra, S. P. Ram, S. K. Tiwari, and S. C. Mehendale, *Phys. Rev. A* **77**, 065402 (2008).